Studii şi Cercetări Ştiinţifice 2023, **24** (3), pp. 233 – 247
Chimie şi Inginerie Chimică, Biotehnologii, Industrie Alimentară

Scientific Study & Research
Chemistry & Chemical Engineering, Biotechnology, Food Industry *ISSN 1582-540X*

ORIGINAL RESEARCH PAPER

NATURAL HYDROXYAPATITE AS AN ADSORBENT FOR MICROORGANISMS (MOS) FROM AQUEOUS SYSTEM

Kshama Parajuli[1*], Bibek Gautam[1], Bijaya Laxmi Maharjan[2], Ganga Gharty Chhetri[2]

Tribhuvan University, Kirtipur, Kathmandu, Nepal
[1]Central Department of Chemistry
[2]Central Department of Microbiology

*Corresponding author: kshamaparajuli@yahoo.com

Received: July, 16, 2023
Accepted: September, 26, 2023

Abstract: Natural hydroxyapatite (HAp) was isolated from calcination of waste caprine (goat) bone at 750 °C in muffle furnace. As produced material was characterized by using X-ray Diffraction (XRD) Fourier Transform Infrared (FTIR) spectroscopy and Scanning Electron Microscopy (SEM) analyses and ensured the synthesized material was nano rod hydroxyapatite. The pH_{PZC} value of the HAp was 7.2 as determined by *p*H drift method. Adsorption of four different microorganisms (MOS) (*E. coli*, *A. baumanii*, *S. aureus* and *C. albicans*) onto natural HAp was investigated and found to adsorb onto HAp with the proportions greater than 25 % within the applied concentration ranges. Adsorption kinetics studies showed the adsorption process followed the pseudo-second order kinetics for all investigated MOS. Antimicrobial study revealed that three adsorbed species (*E. coli*, *S. aureus* and *C. albicans*) onto HAp remained viable form while HAp showed good antibacterial activity towards *A. baumanii*. Minimum inhibition concentration (MIC) and minimum biocidal concentration (MBC) values of HAp were found to be 12.5 and 100 $mg \cdot mL^{-1}$ respectively against *A. baumanii*. Thus, thermal treatment of waste bone powder is found to be cost-effective and environment-friendly method for the isolation of natural nano HAp and it can be applied as an adsorbent for different MOS from aqueous solution as well as a potential antibacterial agent.

Keywords: *adsorption kinetics, antimicrobial study, hydroxyapatite, microorganisms, waste bone*

INTRODUCTION

Water is a crucial entity not only for people but also for many other living organisms on the Earth. Human need water for a variety of activities including drinking, washing, recreation, irrigation, etc. [1]. Only 3 % of all surface water is fresh water and hence there are limited water resources for human consumption. Further, due to rising population and industrialization, the world is currently dealing with water contamination and scarcity of clean drinking water [2].

Both anthropogenic activities and natural processes may pollute water bodies with hazardous heavy metals and other contaminants such as different organics and microorganisms (MOS). However, anthropogenic activities including improper sewage drainage discharge and disposal of different kinds waste into surface water resources are the main causes of MOS contamination, particularly pathogen contamination in water. Presence of pathogenic bacteria in drinking water is dangerous since it can lead to a variety of illnesses [3]. Therefore, the consumer should be given access to sufficient clean drinking water.

The very first step in making contaminated water safe for drinking purpose is to get rid from MOS. Chlorination, ozonation, and UV irradiation are some major methods that are applied to disinfect polluted water [4]. Though chlorination is an effective and cheap way to disinfect water pathogens, it can generate many toxic halogenated organics by reacting with organics present in raw water [3]. Further, the application of ozone and UV irradiation techniques to disinfect the polluted water is not only costly but these techniques require electricity. Moreover, people in developing countries cannot afford such costly techniques and hence it is essential to find a cost-effective, sustainable alternative to disinfect the MOS contaminated water.

Adsorption by different materials can be a promising technique because it is considered a simple, cost-effective, and efficient green method for the removal of water contaminants as adsorption technique does not produce sludge or other secondary pollutants. Further, these days, people are interested in adsorption by nanomaterials because of their high adsorption capacity due to its high specific surface area in comparison to other materials. Hence, different nanomaterials, nanocomposite materials may apply for the bacterial adoption from aqueous system. Shah et *al.* [5] used magnetic-coated chitosan adsorbent to remove the gram-positive and gram-negative bacteria from contaminated water. Similarly, Sasidharan et *al*. [6] evaluated coliform removal efficacy of an adsorbent comprising chitosan, silver/silver oxide nanoparticles and polyurethane foam in aqueous system. Likewise, both synthetic and natural hydroxyapatite is being used as an adsorbent for many water pollutants e.g. arsenic, fluoride, etc. [7]. It is also suggested that the microorganisms adsorbed onto the surface of hydroxyapatite (HAp) can show synergetic effect on removal of heavy metals [8]. Moreover, natural HAp showed to form a chemical bond with living tissue easily [9] that ensured its use as an adsorbent for pathogenic MOS from food and food products [10]. However, very limited studies of microbial adsorption especially oral bacteria onto HAp are reported [11 – 13]. Furthermore, natural HAp was obtained effectively from waste bone [14] and it can be applied as one of the important natural renewable feedstocks for sustainable development. Therefore, this study aims to find out the adsorption capacity of natural HAp extracted from waste caprine (goat) bone toward the MOS in aqueous system.

MATERIALS AND METHODS

Materials

Sodium hydroxide (NaOH), hydrochloric acid (HCl), acetone (CH_3COCH_3), sodium chloride (NaCl) buffer tablets were from Merck Life Science Pvt. Ltd. Methylene blue ($C_{16}H_{18}ClN_3S$) was from Qualigens Fine Chemicals (India). Nutrient Agar (NA), Nutrient Broth (NB), Potato Dextrose Agar (PDA) were from HiMedia Laboratories India. All chemicals were used as supplied without purification.

Preparation of HAp and characterizations

Natural HAp was extracted from bio-waste caprine (goat) bone powders through heat treatment in mantle at 100 °C for 3 hrs with 50 mL of 1 M HCl and then 1 M NaOH in order to remove all the protein and collagen attached to the bone followed by calcination at 750 °C with holding time 5 hrs. Thus, produced bone powder was characterized by different scientific tools like XRD (D_2 phase Diffractometer, Bruker, Germany), FTIR (IR Prestige-21, SHIMADZU, Japan), SEM (Hitachi S-7400 FE-SEM, Japan) analyses. Specific surface area and pH_{PZC} value of the material were determined by methylene blue adsorption method and *p*H drift method (Digital Deluxe *p*H meter, MAX electronics, India), respectively.

Preparation of bacterial stock suspensions

E. coli (ATCC 25922), *S. aureus* (ATCC 29213), *A. baumanii* (ATCC 19606) and *C. albicans* (clinical isolate) were obtained from Central Department of Microbiology (CDM, TU). The bacterial isolates were inoculated in NB and fungi in PDA for 24 hrs at 37 °C. The colony forming units per milliliter ($cfu \cdot mL^{-1}$) of the isolates were determined by spread plate method. The optical density (OD) of this stock solution was measured at 550 nm by using colorimeter (CL 157, ELICO, India). From this stock solution, different concentrations of bacterial suspension were prepared by serial dilution method.

Adsorption study

For adsorption isotherm studies, 5 mL of six different concentrations of each MOS into six different tubes were taken and 15 mg of HAp were added to each tube. The tubes were placed in an orbital/linear thermostatic shaking water bath (Grant OLS 200, Grant Instruments (Cambridge) Ltd., England) at 37 °C, for half an hour. After 5 minutes settling, 3.5 mL of the supernatant from each tube was taken out and adding drops of 2.5 N hydrochloric acid optical densities of the supernatant were measured [15]. Control experiment was a tube containing 15 mg hydroxyapatite in distilled sterile water only. For adsorption kinetics studies, 5 mL of each concentration of MOS (*E. coli* (218×10^5 $cfu \cdot mL^{-1}$), *C. albicans* (125×10^5 $cfu \cdot mL^{-1}$), *S. aureus* (27×10^5 $cfu \cdot mL^{-1}$) and *A. baumanii* suspensions (236×10^5 $cfu \cdot mL^{-1}$)) were added to tubes containing 15 mg hydroxyapatite. Control experiments were performed onto HAp treated with distilled and sterile water. All tubes were immersed in a 37 °C water bath and were shaking in a shaker. During the course of shaking, at 5, 15, 25 and 30 mins. test tubes

were withdrawn one by one and OD of the supernatant was determined as described previously.

Antibacterial/Antifungal activity

Antibacterial activity and antifungal activity were determined by well diffusion agar method with different concentrations of HAp solutions taking DMSO as negative control. Finally, NA and PDA plates were incubated at 37 °C for 24 hrs. Zone of Inhibition (ZOI) was measured with the help of ruler after the 24 hrs of incubation [16].

Minimum inhibition concentration (MIC) and minimum biocidal concentration (MBC) study

Minimum inhibition concentrations (MIC) were determined in a 96-well microtiter plate. Bacteria along with different concentrations of antimicrobial agents are inoculated. Bacterial growth was examined after 24 hours incubation followed by addition of dye (Resazurin). Control experiments were performed by using standard antibiotic solutions [17]. Minimum biocidal concentration (MBC) was found out by plating the content of the wells with concentrations higher than the MIC values of sample and standard antibiotic solutions.

RESULTS AND DISCUSSION

Characterizations

The X-ray diffraction peaks of the powder prepared from thermal treatment of waste caprine bone at 750 °C are presented in Figure 1.

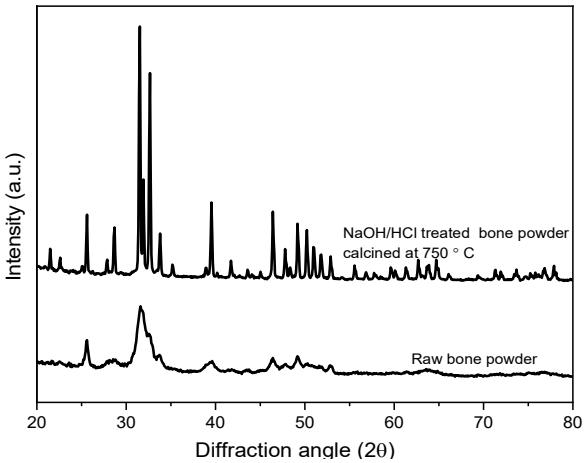

Figure 1. *XRD pattern of the hydroxyapatite powder extracted from waste caprine bone calcined at 750 °C*

Since these peak positions at about 2θ = 26.21, 29.28, 32.12, 32.53, 33.26, 40.16, 47.04, 49.81, 50.84 and 51.61° are nearly resembled to the peak positions of the standard

hydroxyapatite (JCPDS card number 9-0432) suggesting the synthesized particles were hydroxyapatite [18 – 21]. Further, average grain size of the extracted HAp using Debye Scherrer's equation (1) was evaluated as 46 nm:

$$D = \frac{K \times \lambda}{\beta \times cos\theta} \quad (1)$$

where, D is the average crystallite size, K is the broadening constant, λ is the wavelength of Cu Kα radiation (0.15406 nm), β is the full-width at half maximum in radian, and θ is the diffraction angle in degree.

Figure 2 shows the FTIR spectra of the as prepared material. The observed band positions in the spectrum inferred presence of phosphate (PO_4^{3-}) carbonate (CO_3^{2-}) and hydroxide (OH^-) groups in the extracted bone powder [19, 22] and such absorption bands are noticeably visible in powder after thermal treatment than the bone powder without thermal treatment [20]. IR absorption bands appeared at 3572 and 633 cm^{-1} are assigned to OH^- and sharp peaks at 1018 and 1089 cm^{-1} are arisen from asymmetric stretching vibration (v_3) of P-O bond present in PO_4^{3-} group of HAp [23]. Similarly, presence of the bands at 964, 563 and 602 as well as at 471 cm^{-1} referred to v_1 (symmetric stretching), v_4 (bending mode) and v_2 of PO_4^{3-} group respectively. The presence of weak bands at about 1412 cm^{-1} and 1450 cm^{-1} to 1474 cm^{-1} were responsible from CO_3^{2-}. However, these absorption bands due to carbonate groups are sharply reduced after the thermal treatment [16].

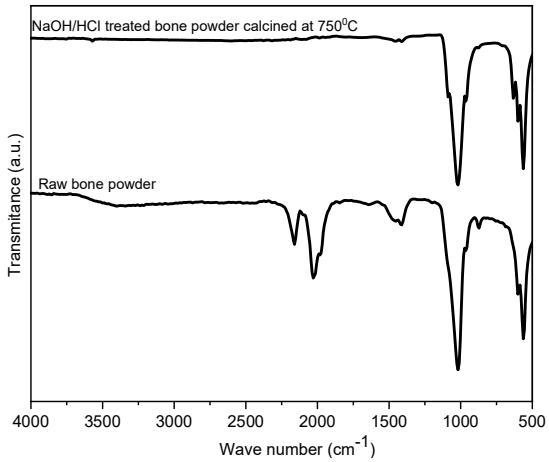

Figure 2. *FTIR spectrum of HAp from caprine bone powders after thermal at 750 ºC*

As depicted in the Figure 3, the isolated HAp particles had inhomogeneous rough surface with agglomeration and were rod shaped with different sizes. Further, obtained SEM images are in agreement with literatures [16, 24].

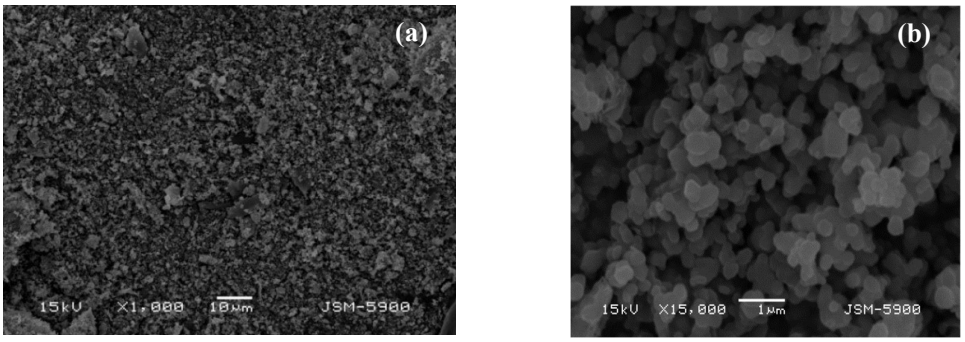

Figure 3. *SEM images of extracted HAp from caprine (goat) bone powder a) low magnification b) high magnification*

Methylene blue adsorption method [25] was applied to determine the specific surface area of the isolated HAp. For this, the adsorption experiments were performed by taking different initial concentration (50, 100, 150, 200, 250, 300 $mg \cdot L^{-1}$) of methylene blue, as an adsorbate and the required amount of the isolated HAp as an adsorbent in a container and then keeping the container in mechanical shaker for 24 hrs to attain equilibrium adsorption. Amount of adsorbate adsorbed at the equilibrium time was evaluated using equation (3) and with the help of obtained equilibrium adsorption data, the linearized Langmuir adsorption isotherm plot (equation 6) for methylene blue was drawn.
Moreover, applying equation 2, observed specific surface area of as prepared HAp was determined and found as 145 $m^2 \cdot g^{-1}$ while the specific surface area of activated carbon was reported to be 499 $m^2 \cdot g^{-1}$ by the same method [26]. The Langmuir surface area of HAp derived from bone scales with average size 13 nm was of about 167 $m^2 \cdot g^{-1}$ [27].

$$S_{MB} = \frac{Ng \times a_{MB} \times N \times 10^{-2}}{M} \quad (2)$$

where S_{MB} is specific surface area, Ng is equivalent to Qm of the Langmuir equation, a_{MB} is the surface area of one molecule of methylene blue, M is molecular weight of methylene blue and N is Avogardo's number.
Point of zero charge (pH_{PZC}) of a material refers to the *p*H value of the medium at which there will be no any charge on its surface. To calculate the pH_{PZC} of the extracted HAp, a graph between changes in (ΔpH) against initial *p*H was plotted as shown in Figure 4.

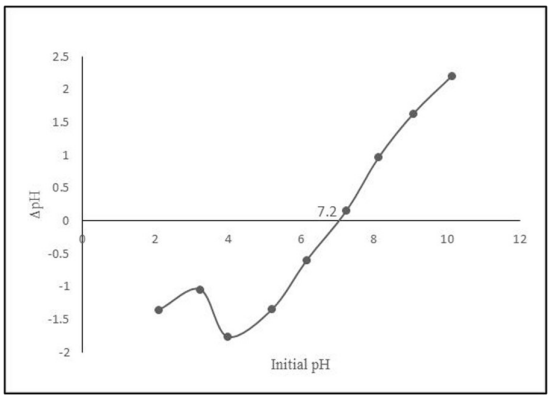

Figure 4. *ΔpH against initial pH for pH_{PZC} measurement of the isolated HAp by pH drift method*

In this study, the pH_{PZC} value of the isolated HAp was found to be 7.2 meaning HAp does not carry any positive or negative charge at *p*H 7.2. Kongsri *et al.* [26] reported the slightly higher pH_{PZC} value of the HAp extracted from fish scale than present study. Moreover, the pH_{PZC} value obtained in the present study was in accordance with the standard value where pH_{PZC} value for HAp was found to be in the range of 6.4 - 8.5 as it depends upon the condition of preparation, washing and storage of apatite materials [27].

Batch adsorption study

The adsorption study of different MOS onto the isolated HAp was carried out by taking the different initial concentrations MOS as described in the experimental section. Amount of bacteria adsorbed per mg of HAp and % of adsorption was evaluated by equations 3 and 4 respectively. The % of adsorption for *E. coli*, *C. albicans*, *S. aureus*, *A. baumanii* was found to be (24.52), (68.94), (46.60), (41.73) respectively. Such variation in % *adsorption results* may be due to many reasons such as initial concentration of MOS taken and also MOS surface compositions and characteristics etc.

$$(Q_e) = \frac{(C_i - C_e) \times 10^5}{M} \times V \quad [\text{cfu}\cdot\text{mg}^{-1}] \tag{3}$$

$$A(\%) = \frac{(C_i - C_e)}{C_i} \times 100 \tag{4}$$

where, C_i = Initial concentration of MOS in cfu·mL^{-1}, C_e = Equilibrium concentration of MOS in cfu·mL^{-1}, M = Amount of adsorbent (HAp) used in mg, V = Volume of microbial suspension in mL. Further, plot of amount of MOS adsorbed at equilibrium (Qe) against bacterial equilibrium concentration (Ce) (Figure 5) was drawn.

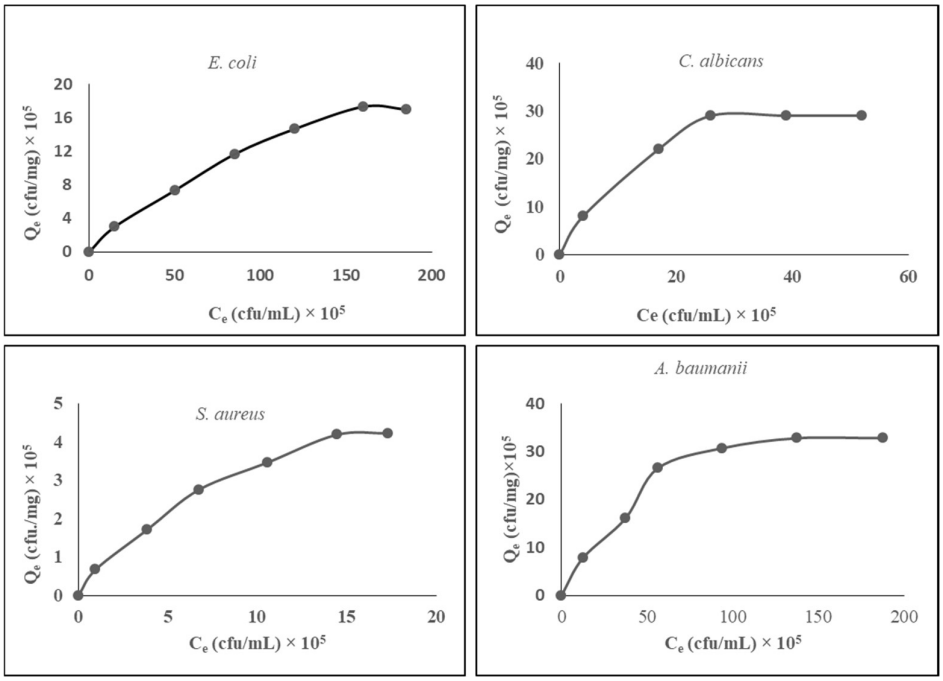

Figure 5. *Plots of amount of MOS adsorbed (Qe) against equilibrium concentration (Ce) onto HAp*

It is seen from the plots that the adsorption of MOS on HAp increases linearly up to certain equilibrium microbial concentration then a plateau is formed and beyond plateau, no further microbial adsorption has been happened since most of the vacant adsorption sites of HAp are covered by MOS. Similar nature of results are reported when by Sasidharan et *al.* [6].

Further, observed equilibrium adsorption data were utilized to fit the linearized Freundlich (equation 5) and Langmuir (equation 6) isotherm model respectively by the least square method [28].

$$\log Q_e = \log K_F + \frac{1}{n}\log C_e \quad (5)$$

$$\frac{C_e}{Q_e} = \frac{1}{Q_m b} + \frac{1}{Q_m} C_e \quad (6)$$

On plotting logQe versus $\log C_e$ (Figure 6), a straight-line plot with intercept (Kf) and slope (1/n) can be obtained. Similarly, a linear Langmuir plot (Figure 7) was drawn by plotting of $\frac{C_e}{Q_e}$ against C_e.

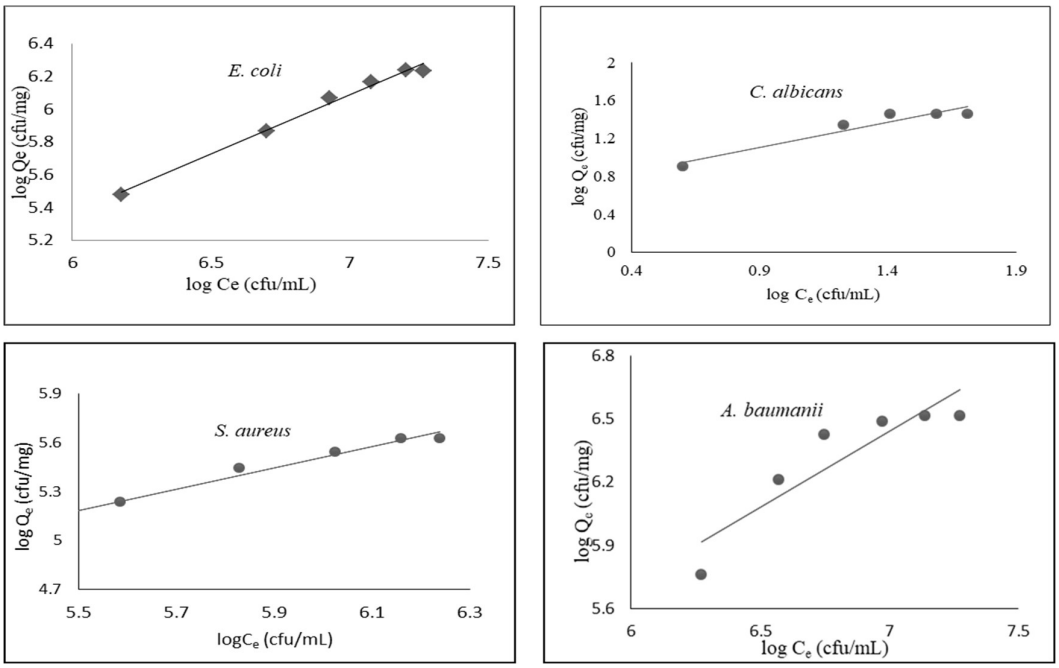

Figure 6. *Linearized Freundlich plot (logQe versus logCe) for different MOS onto HAp*

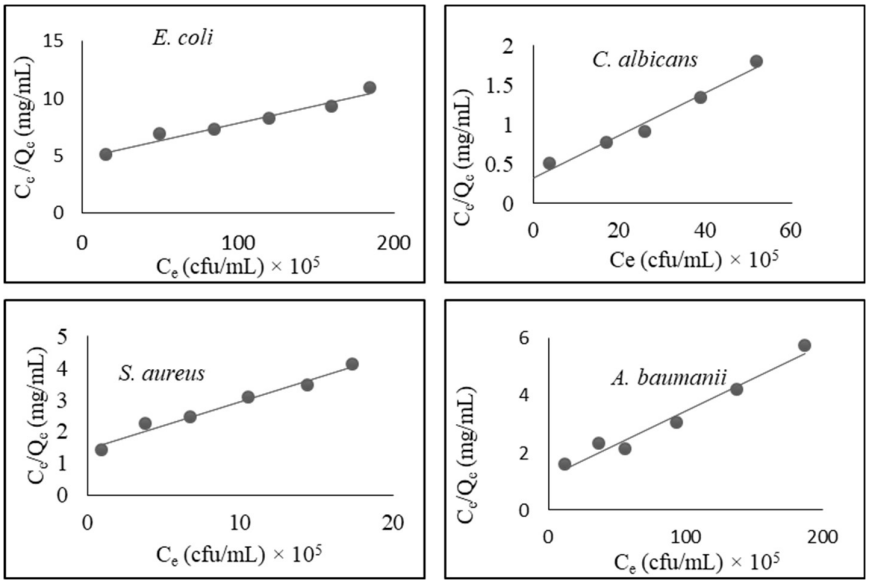

Figure 7. *Linearized Langmuir plot (Ce/Qe versus Ce) for different MOS onto HAp*

Extracted isotherm parameters are summarized in Table 1.

Table 1. *Evaluated isotherm parameters from fitted Langmuir and Freundlich plot for different MOS onto HAp*

Microorganisms	Langmuir parameters			Freundlich parameters		
	Q_m [cfu·mg^{-1}]	b [mL·cfu^{-1}]	R^2	1/n [mg·mL^{-1}]	log K_f [cfu·mg^{-1}]	R^2
E. coli	32.6×10^5	6.5×10^{-8}	0.96	0.72	1.03	0.99 (fit)
C. albicans	34.0×10^5	8.0×10^{-8}	0.97 (fit)	0.53	0.62	0.92
S. aureus	6.7×10^5	1.03×10^{-6}	0.96	0.65	1.59	0.99 (fit)
A. baumanii	43.5×10^5	5.02×10^{-7}	0.97 (fit)	0.73	1.36	0.83

Seeing the (R^2) value, it is suggested that the adsorption of *E. coli* and *S. aurous* onto HAp followed the Freundlich isotherm model while the adsorption of *C. albicans* and *A. baumini* followed the Langmuir isotherm model [5]. Further the 1/n values for all the investigated MOS lie between 0 and 1 inferring the viable adsorption of MOS onto the isolated HAp [29].

Adsorption kinetics study

To see kinetics of MOS onto HAp, adsorption study of MOS was performed by the varying contact time alone and keeping all other parameters constant (Figure 8). Figure 8a shows the amount of MOS adsorbed (Qt) onto HAp as a function of time (t). It is seen that the amount of MOS (adsorbate) adsorbed onto HAp (adsorbent) increases linearly at first because of availability of bigger number of adsorption sites and then gradually increases until it attains equilibrium, beyond which no considerable increase in adsorption of MOS took place because of most of adsorption sites got occupied. The nature adsorption as function of time is consistent with previous studies [5, 6].

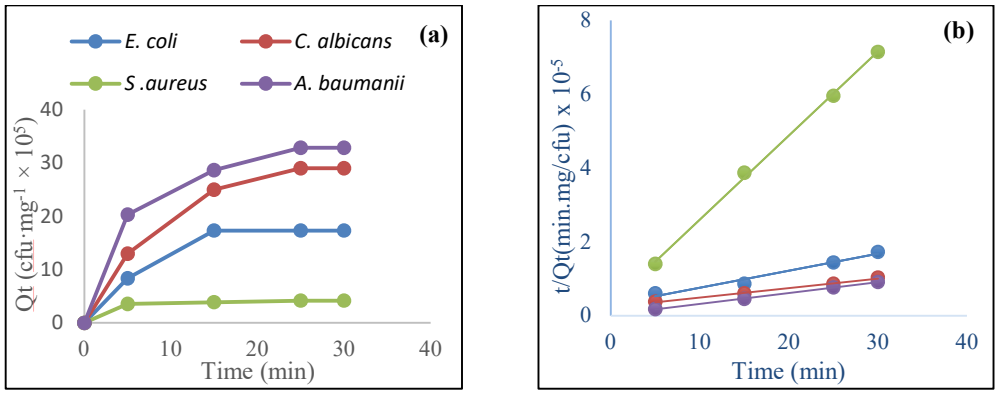

Figure 8. *Kinetic study plots: (a) Plot of MOS adsorbed (Q_t,) against time (b) A plot of pseudo - second order kinetic model for the adsorption of MOS onto HAp*

Further the observed kinetics data were modeled by using pseudo-first order (equation 7) [30] and pseudo-second order (equation 8) [31] kinetics models.

$$\text{Log}(Q_e\text{-}Q_t) = \text{log}Q_e\text{-}\frac{k1}{2.303}\,t \tag{7}$$

$$\frac{t}{Q_t} = \frac{1}{Q_e^2 k_2} + \frac{t}{Q_e} \tag{8}$$

where k_1 and k_2 are pseudo-first order and pseudo-second order rate constants. The pseudo-second order kinetics plot is shown in Figure 8b and Table 2 summaries some extracted kinetic parameters for both models along with correlation coefficient (R^2).

Table 2. *Adsorption kinetics result of different investigated MOS onto HAp*

Microorganism	MOS initial concentration [cfu·mL^{-1}] × 10^5	Time required for maximum adsorption [min]	R^2	
			2nd order	1st order
E. coli	212	15	0.97	0.68
C. albicans	126	25	0.99	0.96
S. aureus	27	5	0.99	0.93
A. baumanii	236	25	0.99	0.93

As can be seen from the Table 2, present kinetic study followed the pseudo-second order kinetics model by all investigated MOS [5].

Microbial activity

To know whether adsorbed MOS onto HAp are viable or not, antibacterial and antifungal test of the isolated HAp against studied MOS was performed. Among the tested MOS, the antibacterial effect of HAp was pronounced only in *A. baumanii*. Hence other studied bacteria and fungus that were adsorbed onto HAp surface were in viable form.
Further, the zone of inhibition was found to be substantially increased as concentration of HAp increased (Figure 9).

Figure 9. *Antibacterial activity of HAp upon A. baumanii*

Larger zone of inhibition signifies the greater number of bacteria killed by HAp. Observed antibacterial effect of HAp, against *A. baumanii* could be due to its thinner cell wall structure in comparison to other investigated MOS. Besides, the surface defects and aggregates on hydroxyapatite particles may make an abrasive surface ordering on HAp surfaces and these were correlated to the mechanical damage of bacterial cell membrane and hence the death of the bacteria [32]. But, to derive the concrete conclusion for the observed antibacterial effect, further studies are suggested.

Minimum inhibition concentration (MIC) and minimum biocidal concentration (MBC) study

Hydroxyapatite showed the antimicrobial property towards the *A. baumanii* (ATCC 19606) which was confirmed from the antimicrobial screening test. To know MIC and MBC value of HAp against this bacterium, another test in sterile 96 well plate was carried out as depicted from Figure 10.

HAp (mg/mL)	Antibiotic (mg/mL)
200	0.25
100	0.125
50	0.0625
25	0.0312
12.5 (MIC)	0.0156 (MIC)
6.25	0.008
3.125	0.004
1.625	0.002

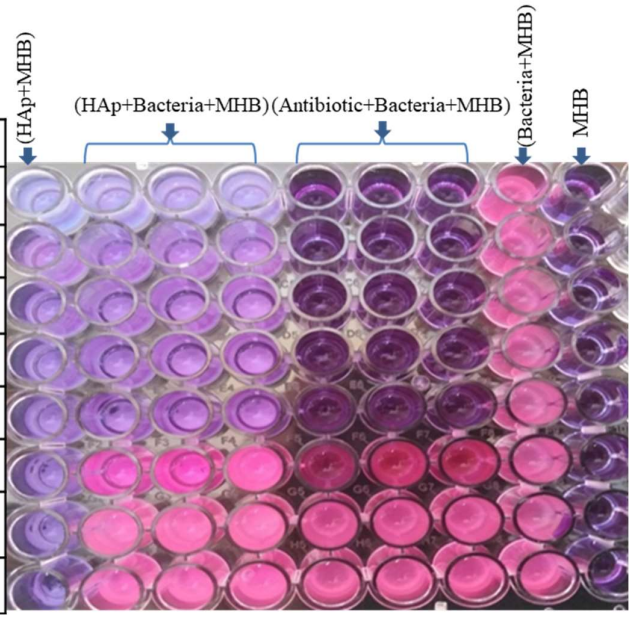

Figure 10. *MIC determination of HAp in sterile 96 well plate using Resazurin as a redox indicator*

MIC value of synthesized HAp against *A. baumanii* was found to be 12.5 mg·mL^{-1} while the standard antibiotic solution showed 0.0156 mg·mL^{-1}. Above this MIC value, HAp could inhibit the bacterial growth so that the initial purple color of Resazurin did not change into final pink color of Resorufin due to the absence of NADH dehydrogenase enzyme. MBC is calculated by culturing the solution from the well having ≥ MIC value of HAp and antibiotic in NA plate as shown in Figure 11.

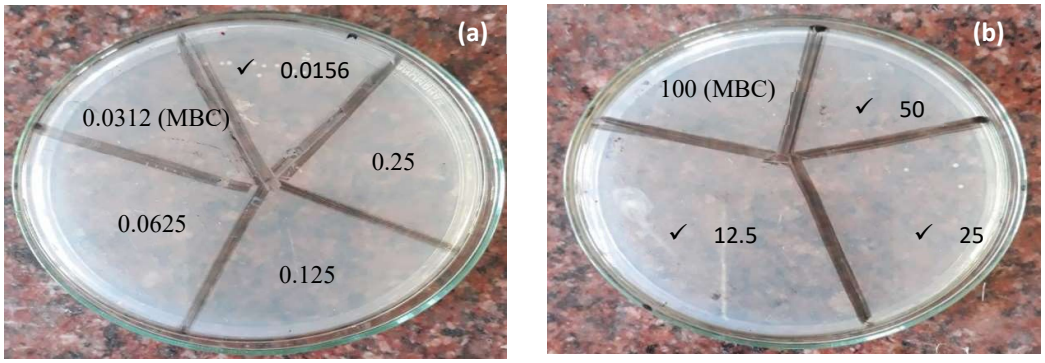

Figure 11. *Photographs showing different concentrations of (a) antibiotic solutions and (b) HAp for the determination MBC*

MBC value of synthesized HAp against *Acinetobacter baumanii* was found to be 100 mg·mL^{-1} while the standard antibiotic solution showed 0.0312 mg·mL^{-1}. Above this MBC value, HAp could kill the bacteria as confirmed by the absence of colony in NA plate as shown in Figure 11. However, below the MBC value, there were bacterial colonies showing the survival of bacteria. The synthesized HAp had though little

antimicrobial property as compared to the antibiotic solution, it can be applicable as sustainable antibacterial agent being cost-effective natural.

CONCLUSIONS

All the organic impurities present in waste caprine bone powder were removed via thermal treatment at 750 °C as observed in the FTIR spectrum. XRD result confirmed that the prepared material was the nano HAp. The isolated HAp had rod shaped, agglomerated structure as seen in SEM images. Specific surface area of the prepared material was 145 $m^2 \cdot g^{-1}$ as found from methylene blue adsorption method and pH_{PZC} of the HAp was found to be 7.2 by *p*H drift method. Extracted HAp was applied as an adsorbent for different microorganisms in aqueous media and adsorption percentage was found to be 25, 69, 47, 42 for *E. coli*, *C. albicans*, *S. aureus* and *A. baumanii* respectively at *p*H 7 and applied concentration ranges. The adsorption process was found to follow Freundlich adsorption isotherm by *E. coli* and *S. aureus* while and Langmuir adsorption isotherm by *C. albicans* and *A. baumanii*. Adsorption kinetics studies showed that the contact time required for maximum adsorption fell within 25 minutes and follow pseudo-second order kinetics for all studied microorganisms. Antimicrobial study revealed that three adsorbed species (*E. coli*, *S. aureus* and *C. albicans*) onto HAp remained viable while HAp showed good antibacterial activity towards *A. baumanii*. MIC and MBC values of HAp were found to be 12.5 and 100 $mg \cdot mL^{-1}$ respectively against *A. baumanii*. Hence, thermal treatment of waste caprine bone powder is a cheap and sustainable method for the isolation of natural nano HAp. Moreover, it can be applied as a potential adsorbent for different MOS from aqueous system as well as an efficient antibacterial agent.

REFERENCES

1. Hossain, M.Z.: Water: The Most Precious Resource of Our Life, *Global Journal of Advanced Research*, **2015**, **2** (9), 1436-1445;
2. Aziz, A., Akram, K., Abrar ul Haq, M., Hawaldar, I.T., Rabbani, M.R.: Examining the Role of Clean Drinking Water Plants in Mitigating Drinking Water-Induced Morbidity, *Sustainability*, **2022**, **14** (15), 9644, https://doi.org/10.3390/su14159644;
3. Hemdan, B.A., El-Taweel, G.E., Goswami, P., Pant, D., Sevda, S.: The Role of Biofilm in the Development and Dissemination of Ubiquitous Pathogens in Drinking Water Distribution Systems: An Overview of Surveillance, Outbreaks, and Prevention, *World Journal of Microbiology and Biotechnology*, **2021**, **37** (2), 36, https://doi.org/10.1007/s11274-021-03008-3;
4. Mezzanotte, V., Antonelli, M., Citterio, S., Nurizzo, C.: Wastewater Disinfection Alternatives: Chlorine, Ozone, Peracetic Acid, and UV Light, *Water Environment Research*, **2007**, **79** (12), 2373-2379;
5. Shah, K.H., Yameen, M.A., Yousaf, T., Waseem, M., Fahad, M., Sherazi, T.A., Ahmad, M.: Adsorption of Bacteria by Highly Efficient, Economic and Biodegradable Magnetic Coated Chitosan Adsorbent, *Journal of Solution Chemistry*, **2020**, **49** (11), 1304-1318;
6. Sasidharan, A.P., Meera, V., Raphael, V.P.: Coliform Removal Efficacy of Polyurethane Foam Impregnated with Chitosan Nanoparticles and Silver/Silver Oxide Nanoparticles, *Water Supply*, **2022**, **22** (5), 5675-5687;
7. Alkurdi, S.S.A., Al-Juboori, R.A., Bundschuh, J., Bowtell, L., McKnight, S.: Effect of Pyrolysis Conditions on Bone Char Characterization and Its Ability for Arsenic and Fluoride Removal, *Environmental Pollution*, **2020**, **262**, 114221, https://doi.org/10.1016/j.envpol.2020.114221;

8. Piccirillo, C., Pereira, S.I.A., Marques, A.P.G.C., Pullar, R.C., Tobaldi, D.M., Pintado, M.E., Castro, P.M.L.: Bacteria Immobilisation on Hydroxyapatite Surface for Heavy Metals Removal, *Journal of Environmental Management*, **2013**, **121**, 87-95;
9. Barakat, N.A.M., Khil, M.S., Omran, A.M., Sheikh, F.A., Kim, H.Y.: Extraction of Pure Natural Hydroxyapatite from the Bovine Bones Bio Waste by Three Different Methods, *Journal of Material Processing Technology*, **2009**, **209** (7), 3408-3415;
10. Berry, E.D., Siragusa, G.R.: Hydroxyapatite Adherence as a Means to Concentrate Bacteria, *Applied and Environmental Microbiology*, **1997**, **63** (10), 4069-4074;
11. Clark, W.B., Gibbons, R.J.: Influence of Salivary Components and Extracellular Polysaccharide Synthesis from Sucrose on the Attachment of *Streptococcus mutans* 6715 to Hydroxyapatite Surfaces, *Infection and Immunity*, **1977**, **18** (2), 514-523;
12. Clark, W.B., Lane, M.D., Beem, J.E., Bragg, S.L., Wheeler, T.T.: Relative Hydrophobicities of *Actinomyces viscosus* and *Actinomyces naeslundii* Strains and Their Adsorption to Saliva-Treated Hydroxyapatite, *Infection and Immunity*, **1985**, **47** (3), 730-736;
13. Cowan, M.M., Taylor, K.G., Doyle, R.J.: Energetics of the Initial Phase of Adhesion of *Streptococcus sanguis* to Hydroxylapatite, *Journal of Bacteriology*, **1987**, **169** (7), 2995-3000;
14. Malla, K.P., Regmi, S., Nepal, A.; Bhattarai, S., Yadav, R.J., Sakurai, S., Adhikari, R.: Extraction and Characterization of Novel Natural Hydroxyapatite Bioceramic by Thermal Decomposition of Waste Ostrich Bone, *International Journal of Biomaterials*, **2020**, **2020**, 1690178, https://doi.org/10.1155/2020/1690178;
15. O'Brien, W.J., Fan, P.L., Loesche, W.J., Walker, M.C., Apostolids, A.: Adsorption of Streptococcus Mutans on Chemically Treated Hydroxyapatite, *Journal of Dental Research*, **1978**, **57** (9-10), 910-914;
16. Parajuli, K., Malla, K.P., Panchen, N., Ganga, G.C., Adhikari, R.: Isolation of Antibacterial Nano-Hydroxyapatite Biomaterial from Waste Buffalo Bone and Its Characterization, *Chemistry and Chemical Technology*, **2022**, **16** (1), 133-141;
17. Elshikh, M., Ahmed, S., Funston, S., Dunlop, P., McGaw, M., Marchant, R., Banat, I.M.: Resazurin-Based 96-Well Plate Microdilution Method for the Determination of Minimum Inhibitory Concentration of Biosurfactants, *Biotechnology Letter*, **2016**, **38**, 1015-10195;
18. Bahrololoom, M.E., Javidi, M., Javadpour, S., Ma, J.: Characterisation of Natural Hydroxyapatite Extracted from Bovine Cortical Bone Ash, *Journal of Ceramic Processing Research*, **2009**, **10** (2), 129-138;
19. Ooi, C.Y., Hamdi, M., Ramesh, S.: Properties of Hydroxyapatite Produced by Annealing of Bovine Bone, *Ceramic International*, **2007**, **33** (7), 1171-1177;
20. Khoo, W., Nor, F.M., Ardhyananta, H., Kurniawan, D.: Preparation of Natural Hydroxyapatite from Bovine Femur Bones Using Calcination at Various Temperatures, *Procedia Manufacturing*, **2015**, **2**, 196-201;
21. Ofudje, E.A., Rajendran, A., Adeogun, A.I., Idowu, M.A., Kareem, S.O., Pattanayak, D.K.: Synthesis of Organic Derived Hydroxyapatite Scaffold from Pig Bone Waste for Tissue Engineering Applications, *Advanced Powder Technology*, **2018**, **29** (1), 1-8;
22. Walters, M.A., Leung, Y.C., Blumenthal, N.C., Konsker, K.A., LeGeros, R.Z.: A Raman and Infrared Spectroscopic Investigation of Biological Hydroxyapatite, *Journal of Inorganic Biochemistry*, **1990**, **39** (3), 193-200;
23. Markovic, M.: Preparation and Comprehensive Characterization of a Calcium Hydroxyapatite Reference Material, *Journal of Research of the National Institute of Standards and Technology*, **2004**, **109** (6), 553-568;
24. Shavandi, A., Bekhit, A.E.D.A., Ali, A., Sun, Z.: Synthesis of Nano-Hydroxyapatite (nHA) from Waste Mussel Shells Using a Rapid Microwave Method, *Materials Chemistry and Physics*, **2015**, **149-150**, 607-616;
25. Jha, P.K., Jha, V.K.: Arsenic Adsorption Characteristics of Adsorbent Prepared from *Spinacia oleracea* (Spinach) Leaves, *Scientic World*, **2021**, **14** (14), 51-61;
26. Kongsri, S., Janpradit, K., Buapa, K., Techawongstien, S., Chanthai, S.: Nanocrystalline Hydroxyapatite from Fish Scale Waste: Preparation, Characterization and Application for Selenium Adsorption in Aqueous Solution, *Chemical Engineering Journal*, **2013**, **215-216**, 522-532;
27. Bell, L.C., Posner, A.M., Quirk, J.P.: The Point of Zero Charge of Hydroxyapatite and Fluorapatite in Aqueous Solutions, *Journal of Colloid and Interface Science*, **1973**, **42** (2), 250-261;

28. Karmacharya, M.S, Gupta, V.K., Jha, V.K.: Preparation of Activated Carbon from Waste Tire Rubber for the Active Removal of Cr (VI) and Mn (II) Ions from Aqueous Solution, *Transactions of the Indian Ceramic Society*, **2016**, **75** (4), 234-241;
29. Parajuli, K., Sah, A.K., Paudyal, H.: Green Synthesis of Magnetite Nanoparticles Using Aqueous Leaves Extracts of *Azadirachta indica* and Its Application for the Removal of As(V) from Water, *Green and Sustainable Chemistry*, **2020**, **10** (04), 117-132;
30. Lagergren, S.: Zur Theorie der Sogenannten Adsorption Gelöster Stoffe, *Kungliga Svenska Vetenskapsakademiens, Handlingar*, **1898**, **24** (4), 1-39;
31. Ho, Y.S., McKay, G.: Pseudo-Second Order Model for Sorption Processes, *Process Biochemistry*, **1999**, **34** (5), 451-465;
32. Resmim, C.M., Dalpasquale, M., Vielmo, N.I.C., Mariani, F.Q., Villalba, J.C., Anaissi, F.J., Caetano, M.M., Tusi, M.M.: Study of Physico-Chemical Properties and in vitro Antimicrobial Activity of Hydroxyapatites Obtained from Bone Calcination, *Progress in Biomaterials*, **2019**, **8** (1), 1-9, https://doi.org/10.1007/s40204-018-0105-2.